Available online at www.sciencedirect.com
SCIENCE DIRECT®
ELSEVIER
Earth and Planetary Science Letters 214 (2003) 27–42
EPSL
www.elsevier.com/locate/epsl

Volatiles (nitrogen, noble gases) in recently discovered SNC meteorites, extinct radioactivities and evolution ☆

K.J. Mathew [a,*], B. Marty [a,b,c], K. Marti [a], L. Zimmermann [b]

[a] *Department of Chemistry and Biochemistry, University of California, San Diego, La Jolla, CA 92093-0317, USA*
[b] *CRPG, BP 20, 54501 Vandoeuvre lès Nancy Cedex, France*
[c] *Ecole Nationale Supérieure de Géologie, Rue du Doyen Roubault, 54501 Vandoeuvre Cedex, France*

Received 25 February 2003; received in revised form 20 June 2003; accepted 24 June 2003

Abstract

We report noble gas and nitrogen analyses of newly discovered SNC meteorites, one nakhlite (NWA817) and four shergottites (NWA480, NWA856, NWA1068, and SaU 005). The K–Ar age (1.3 Ga) as well as the cosmic-ray exposure (CRE) age (10.0 ± 1.3 Ma) of nakhlite NWA817 agree with data of Nakhla. The CRE ages of NWA480, NWA856, and NWA1068 (2.35 ± 0.20, 2.60 ± 0.21 and 2.01 ± 0.65 Ma, respectively) are consistent, within uncertainties, with other basaltic shergottites, but the CRE age of SaU 005 (1.25 ± 0.07 Ma) is distinct and indicates a different ejection event. Bulk K–Ar ages of all shergottites exceed the reported radiometric ages and reveal the presence of inherited radiogenic ^{40}Ar in basaltic lavas. The isotopic composition of nitrogen trapped in these SNC meteorites is not homogeneous, since δ^{15}N values of either +15 to 20‰ or +45‰, indicate different nitrogen reservoirs. All shergottites contain fission xenon from ^{238}U, and fission Xe of extinct ($T_{1/2}$ = 82 Ma) ^{244}Pu, previously identified in ALH84001, in Chassigny and in Nakhla is also present in at least one shergottite (NWA856). The shergottites contain less fissiogenic Xe than other SNC, suggesting that either their source was more degassed or that the magma source region closed at a later time. In nakhlites, fission xenon from ^{244}Pu correlates with uranium, a geochemical proxy of plutonium. Thus it is possible that fissiogenic Xe was not inherited during magma differentiation, but rather was produced in situ and retained in refractory mineral assemblages. In this interpretation, the magma evolution that settled the mineralogy and geochemistry of nakhlites took place at a time when ^{244}Pu was alive and pre-dated the (late) events recorded in their radiometric ages. Alternatively, fissiogenic xenon was trapped from a mantle source during closed system evolution of the parent magmas, in which case such evolution might have taken place at considerable depth (pressure) in order to inhibit magma degassing during the course of differentiation.

Keywords: Mars; SNC meteorites; volatiles; atmosphere; nitrogen; noble gases

* Corresponding author. Tel.: +1-858-534-0443; Fax: +1-858-534-7441.
E-mail address: mkattath@ucsd.edu (K.J. Mathew).

☆ Supplementary data associated with this article can be found at doi: 10.1016/S0012-821X(03)00365-0

0012-821X/03/$ – see front matter
doi:10.1016/S0012-821X(03)00365-0

1. Introduction

Chronologies based on extinct radionuclides in Martian meteorites established that Mars was accreted on time scales of several Ma [1,2]. Constraints on the early evolution of Martian volatiles were obtained from the interior reservoirs (light N and solar 'Chass-S' Xe components) sampled by the Martian meteorite Chassigny [3,4] and from signatures of an evolved (assimilated fission gas and radiogenic $^{129}Xe_r$) Xe component in ALH84001 [4,5] and in Nakhla [6–9]. Marty and Marti [10] argued that the presence of fission Xe from ^{244}Pu in Mars is evidence that (i) fission Xe in the Martian mantle was not lost, demonstrating different geodynamic regimes between the planets Earth and Mars, and (ii) this extinct radionuclide signature survived the resetting events recorded in ^{40}K–^{40}Ar, ^{87}Rb–^{87}Sr and ^{147}Sm–^{143}Nd ages of Chassigny and nakhlites.

The ratios $^{129}Xe/^{132}Xe > 2$ observed in the 700–1000°C fractions of Nakhla were identified to represent a rather recent atmospheric component exhibiting the signature of mass-fractionated Xe [6]. Further, $^{129}Xe_{rad}$ excesses relative to Chass-S xenon are observed in nakhlites and also in shergottites [3,6–9,11–13]. The Xe signatures observed in ALH84001 were interpreted to represent an ancient atmospheric signature that prevailed ~3.95 Ga ago [4,5]. Identifications of paleoatmospheric components are essential for an assessment of changes brought about by the period of heavy bombardment which was implicated to be responsible for the warming and melting of subsurface ice and the creation of valley network on Mars [14].

Nyquist et al. [15] reviewed the chronology of 16 Martian meteorites (11 shergottites, subdivided into eight basaltic and three lherzolitic, three nakhlites, Chassigny, and the ALH84001 orthopyroxenite). These authors subdivided the shergottites based on their crystallization ages of ~175 and 330–475 Ma. The nakhlites and Chassigny have distinct crystallization ages of ~1.3 Ga, while ALH84001 crystallized ~4.5 Ga ago, but has a metamorphic age of ~3.9 Ga. The Martian meteorites have also been grouped on the basis of their ejection ages [16], and these data for the shergottites currently require four events, while a single ejection event is indicated for the nakhlites. The number of distinct ejection events indicated by the cosmic-ray exposure (CRE) ages of SNC meteorites conflict with those based on radiochronology (see Nyquist et al. [15]).

2. Experimental procedures

2.1. Sample description

2.1.1. Nakhlite NWA817

North West Africa 817 is an unbrecciated, olivine-bearing clinopyroxenite with a cumulate texture [17]. The mesostasis consists of feldspars with trace amounts of sulfides, Ti-magnetite and acicular pyroxene. Alteration products similar to those described in other nakhlites are observed, which, however, have lower Al and higher Fe content.

2.1.2. Shergottite NWA480

North West Africa 480 is an Al-poor ferroan basaltic shergottite that resembles Zagami and Shergotty [18]. The compositional trend of pyroxenes may indicate that NWA480 formed from a melt with a low nuclei density at a slow cooling rate as proposed for QUE94201 [19].

2.1.3. Shergottite NWA856

This basaltic shergottite (320 g) has an REE pattern similar to Shergotty and Zagami [20]. Minor minerals identified are merrilite, apatite, pyrrhotite, chromite, Fe–Ti oxides, stishovite and baddeleyite.

2.1.4. Shergottite NWA1068

North West Africa 1068 is a new picritic shergottite (577 g) [21] with REE similar to those of Shergotty, Zagami, and Los Angeles. Trace element abundances demonstrate that it is not paired with any other hot desert finds and may derive from a basaltic shergottite which has accumulated and partly digested fragments of olivine-rich lithology.

2.1.5. Shergottite SaU 005 (Sayh al Uhaymir 005)

SaU 005 is basaltic, with affinity to lherzolitic shergottite. Dreibus et al. [22] reported bulk composition of this meteorite and Pätsch et al. [23] reported a noble gas-based exposure age of 1.5 Ma and a K–Ar age of ~1 Ga.

2.2. Mass spectrometry

Small chips (~10 mg) of the meteorites were taken and analyzed at CRPG, Nancy, for the light noble gases He, Ne and Ar, as well as ^{132}Xe abundances and ^{129}Xe/^{132}Xe ratios. The CRPG data also served as pilot samples for the stepwise release studies of N, Ar, and Xe in larger (100–300 mg) samples at UCSD. In all cases interior chips were used for the analyses.

Sample fragments were ultrasonically cleaned in analytical-grade acetone and loaded in a sample chamber where they were baked overnight at a temperature of 100°C. They were left under vacuum for 3 weeks before analysis, to allow further degassing of terrestrial contamination. Samples were heated using a defocused CO_2 laser in one (~1600°C) or two (~700°C and 1600°C) temperature steps and were analyzed by static mass spectrometry using previously described procedures [24]. During this study, blanks at CRPG were $2.0 \pm 0.7 \times 10^{-10}$ cm^3 STP for ^{4}He, $6.0 \pm 1.5 \times 10^{-12}$ cm^3 STP for ^{20}Ne, $2.0 \pm 0.2 \times 10^{-12}$ cm^3 STP for ^{36}Ar, and $1.3 \pm 0.8 \times 10^{-13}$ cm^3 STP for ^{132}Xe.

The nakhlite NWA817, shergottites NWA856, NWA1068 (two chips), and SaU 005 were loaded into the gas extraction system at UCSD without wrapping. Shergottite NWA480 was wrapped in pre-degassed Au foil since many small chips were used for analysis. The meteorites were step-heated up to 1000°C in a double-walled quartz system and then transferred in vacuo into a Mo crucible, for step-heating by radio frequency to the melting temperatures. Details of the analysis procedure were described previously [6,25]. A low-temperature combustion (in 3 Torr O_2) was carried out to remove terrestrial contamination. Extraction blanks for N were 0.1–0.4 ng for the ≤1400°C steps and were of atmospheric composition ($\delta^{15}N = 0 \pm 3$ ‰), while typical blanks for ^{36}Ar and ^{132}Xe (also of atmospheric composition) were $1–3 \times 10^{-12}$ cm^{3}STP/g and $1–2 \times 10^{-14}$

Table 1
He and Ne abundances and isotopic ratios in NWA817, NWA856, NWA480, NWA1068, and SaU 005

Temp.	^{3}He	^{3}He/^{4}He	^{20}Ne	^{20}Ne/^{22}Ne	^{21}Ne/^{22}Ne	CRE age (Ma)				
(°C)						^{3}He	^{21}Ne	^{38}Ar	^{15}N	T_{av}
Nakhlite NWA817, 9.3 mg										
700	1442	0.0142(1)	60	0.987(20)	0.824(44)					
1600	44	0.0159(7)	156	0.977(14)	0.824(29)					
Total	1486	0.0142(3)	216	0.994(25)	0.824(53)	8.69	9.28	11.7	10.3	9.99 ± 1.32
Shergottite NWA480, 17.7 mg										
700	396	0.1199(32)	36	1.421(27)	0.749(58)					
1600	5.2	0.0479(86)	53	1.460(25)	0.769(51)					
Total	401	0.1176(39)	89	1.465(36)	0.761(77)	2.36	2.53	2.07	2.42	2.35 ± 0.20
Shergottite NWA856, 9.9 mg										
700	384	0.0254(4)	46	1.436(39)	0.699(35)					
1600	2	0.0227(30)	45	1.555(41)	0.719(36)					
Total	386	0.0254(6)	91	1.514(57)	0.708(50)	2.34	2.86	2.58	2.60	2.60 ± 0.21
Shergottite NWA1068, 7.7 mg										
700	381	0.113(12)	62	4.102(44)	0.579(8)					
1600	51	0.169(25)	50	1.205(11)	0.970(13)					
Total	432	0.118(15)	112			2.41	1.14	1.89	2.60	2.01 ± 0.65
Shergottite SaU 005										
								1.20	1.30	1.25 ± 0.07

The CRE ages based on ^{3}He, ^{21}Ne, ^{38}Ar$_C$, and ^{15}N$_C$ (and their averages) are listed.
The data are corrected for blanks and mass discrimination. The ^{3}He and ^{20}Ne abundances are in units 10^{-10} cm^{3}STP/g.

Table 2
Measured ^{36}Ar concentrations and Ar isotopic ratios (95% confidence limits)

Sample	Temp. (°C)	^{36}Ar	$^{40}Ar/^{36}Ar$	$^{36}Ar/^{38}Ar$	$^{38}Ar_C$	^{132}Xe	$^{129}Xe/^{132}Xe$	$^{36}Ar/^{132}Xe$	$^{84}Kr/^{132}Xe$
Nakhlite	150	0.25	290 ± 20	5.3 ± 0.12		0.10	0.98	246	4.6
NWA817	250	6.20	287 ± 10	5.3 ± 0.06		3.11	0.98	199	4.2
131 mg	350	9.28	664 ± 4	4.58 ± 0.03	0.31	5.93	1.04	153	3.9
	450	9.20	735 ± 5	3.75 ± 0.03	0.82	2.04	1.04	425	4.5
	550	2.47	5 120 ± 8	1.90 ± 0.02	0.95	0.74	1.04	251	6.0
	700	9.11	12 850 ± 18	1.28 ± 0.02	6.15	1.59	1.08	321	6.0
	800	12.50	3 675 ± 8	2.13 ± 0.010	4.00	3.04	1.12	325	6.0
	1000	14.30	1 965 ± 5	2.02 ± 0.008	5.00	21.50	1.17	51	5
	1200	81.00	75.5 ± 3	0.82 ± 0.006	95.17	18.60	1.27	103	4.2
	1400	67.10	20.1 ± 2	0.70 ± 0.006	94.84	2.02	1.64	270	4.2
	1600	1.24	291 ± 9	5.20 ± 0.15		0.50	1.08	247	4.2
	Total	213	1 064	0.958	207.2	59.2	1.18	132	4.6
9.3 mg	700	123	1 813 ± 126	2.95 ± 0.008		31.4	1.13		
	1600	99	151 ± 15	0.61 ± 0.002		30.3	1.26		
	Total	222	1 084	1.085	187.7	61.7	1.19		
Shergottite	250	0.10	292 ± 12	5.30 ± 0.15		0.13	0.98	748	4.2
NWA480	500	2.10	300 ± 8	5.29 ± 0.08		1.27	0.98	166	4.1
186.8 mg	450C	0.17	290 ± 20	5.1 ± 0.3		2.19	0.98	8	4.0
	700	6.07	550 ± 2	4.20 ± 0.04	0.34	2.90	0.98	202	4.5
	900	7.60	1 050 ± 4	1.46 ± 0.01	4.30	2.20	1.08	218	4.3
	1000	2.65	720 ± 3	1.08 ± 0.009	2.23	0.73	1.10	165	4.8
	1200	9.72	558 ± 2	0.75 ± 0.006	12.69	0.97	1.20	152	4.5
	1400	6.78	328 ± 2	1.40 ± 0.011	4.06	2.56	1.25	162	4.3
	1600	1.15	300 ± 10	5.25 ± 0.11		0.87	1.06	132	4.2
	Total	36.3	596	1.34	23.6	13.8	1.07	158	4.0
17.7 mg	700	11	746 ± 44	2.43 ± 0.012		5.8	1.04		
	1600	25	653 ± 19	1.02 ± 0.003		4.5	1.22		
	Total	36	707	1.24	24.6	10.3	1.12		
Shergottite	150	0.43	300 ± 11	5.30 ± 0.12		0.22	0.98	194	4
NWA856	350	0.99	296 ± 8	5.28 ± 0.10		0.42	0.98	237	3.7
84.1 mg	500	2.57	680 ± 4	3.50 ± 0.04	0.28	1.80	0.98	132	3.6
	450C	0.15	290 ± 22	5.30 ± 0.15		0.10	0.98	147	3.5
	1000	13.80	1 630 ± 9	1.32 ± 0.02	8.97	4.0	1.05	200	4.0
	1600	37.80	401 ± 5	1.70 ± 0.02	17.22	21.30	1.07	125	4.2
	Total	55.3	716	1.65	26.5	27.6	1.06	139	4.1
9.9 mg	700	12	1 339 ± 113	2.33 ± 0.011		48.9	1.02		
	1600	29	854 ± 35	1.07 ± 0.003		6.6	1.16		
	Total	41	1 002	1.279	27.7	55.5	1.04		
Shergottite	150	0.14	293 ± 23	5.25 ± 0.15		0.12	0.98	114	4.0
NWA1068	500	2.44	345 ± 15	5.24 ± 0.11		3.02	0.98	81	4.6
287.1 mg	450C	0.06	300 ± 30	5.3 ± 0.2		0.05	1.0	125	8.0
	800	12.70	1 840 ± 11	2.06 ± 0.01	4.29	3.14	1.02	315	4.9
	1000	13.50	1 376 ± 12	1.27 ± 0.01	9.20	2.16	1.12	347	4.0
	1200	9.92	246 ± 2	0.96 ± 0.01	9.65	1.93	1.24	189	4.2
	1600	6.53	264 ± 2	2.80 ± 0.02	1.25	3.65	1.22	157	4.0
	Total	45.3	1 038	1.51	24.4	14.1	1.11	209	4.4
7.7mg	900	46	335 ± 5	3.937 ± 0.06		–	–	–	–
	1600	45	951 ± 15	1.701 ± 0.029		–	–	–	–
	Total	91	638	2.387	23.2	–	–	–	–

Table 2 (*Continued*).

Sample	Temp. (°C)	^{36}Ar	$^{40}Ar/^{36}Ar$	$^{36}Ar/^{38}Ar$	$^{38}Ar_C$	^{132}Xe	$^{129}Xe/^{132}Xe$	$^{36}Ar/^{132}Xe$	$^{84}Kr/^{132}Xe$
Shergottite	150	0.54	296 ± 11	5.27 ± 0.15		0.51	0.99	105	5.2
SaU 005	500	1.07	300 ± 10	5.3 ± 0.11		1.02	0.98	105	5
207.6 mg	450C	0.17	290 ± 22	5.2 ± 0.2		0.08	0.99	216	6.5
	800	7.77	438 ± 2	3.75 ± 0.02	0.72	1.90	0.98	403	6
	1000	5.22	920 ± 3	2.07 ± 0.01	1.75	1.26	1.03	324	4.8
	1400	11.30	255 ± 2	1.20 ± 0.01	8.28	3.89	1.25	151	4
	1600	3.21	221 ± 3	1.60 ± 0.03	1.60	1.81	1.05	120	3.6
	Total	29.3	423.6	1.78	12.4	10.5	1.05	201	4.3

The data are corrected for blanks and mass discrimination. The ^{36}Ar and $^{38}Ar_C$ abundances are in units 10^{-10} cm^3STP/g and the ^{132}Xe abundances are in 10^{-12} cm^3STP/g. C denotes a combustion step in O_2.

cm^3STP/g, respectively. The propagated uncertainties in the isotopic ratios include statistical errors, and uncertainties in the discrimination correction and in blank corrections.

Measured abundances of He and Ne are listed in Table 1, and those of Ar, N, and Xe in Tables 2, 3, and 4, respectively. Since four of the meteorites were measured at CRPG and at UCSD for both Ar and Xe, we have an opportunity for inter-laboratory calibrations. The agreement between the data sets is very good, considering the small sample size (≤ 10 mg) used at CRPG. ^{40}Ar abundances agree within $< 11\%$ and the ^{132}Xe abundances agree within $< 17\%$, except for the ^{132}Xe abundance in NWA856 measured at CRPG, which was about twice as much. However, 88% of ^{132}Xe in this crushed sample is released in the 700°C step and indicates a large atmospheric contamination.

3. Cosmic-ray exposure ages

Some SNC launch models are not consistent with the large number of distinct Martian ejection events indicated by the CRE ages [15]. Head et al. [26] report numerical simulations that suggest that much smaller craters may account for the ejection of SNC meteorites, and that the required minimum size of impactors depends on the target material, specifically the thickness of the regolith layers. Improved statistics on CRE ages of SNCs should help to constrain the number of recent cratering events.

CRE ages of NWA817, NWA480, and NWA856 have been reported in an abstract [27] and the full data set is presented here. For the identification of trapped and cosmogenic Ne, a $(^{20}Ne/^{22}Ne)_t = 10.6$ [11] was adopted (since the data are close to the cosmogenic end-member with $(^{20}Ne/^{22}Ne)_C = 0.8$, adopting a terrestrial ratio of 9.80 yields similar $^{21}Ne_C$ ages). ^3He was assumed to be entirely cosmogenic since observed $^3He/^4He$ ratios are two orders of magnitude higher than the solar value. The high $(^{22}Ne/^{21}Ne)_C$ values of 1.19 (NWA817), 1.31 (NWA856) and 1.22 (NW480) are suggestive of insignificantly shielded meteoroids and, at least in the case of NWA856, may indicate a contribution by SCR in addition to the GCR spallation component. From the Mg/(Si+Al) vs. $(^{21}Ne/^{22}Ne)_C$ diagram

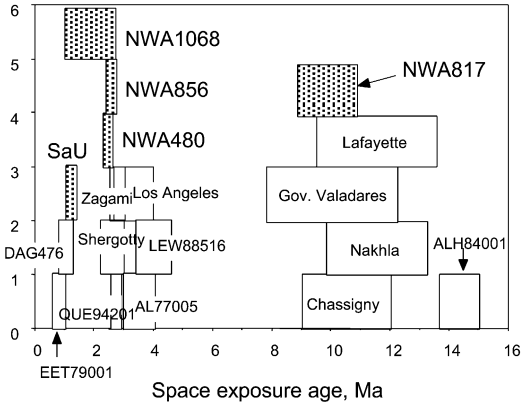

Fig. 1. Space exposure ages of new SNC meteorites studied here (filled bars), compared to published data (open bars, see Eugster et al. [34] for references to literature data).

[28,29], we note that the NWA856 data suggest a significant contribution from SCR. The cosmogenic production rates of ^{3}He, ^{21}Ne, and ^{38}Ar, (P_3, P_{21}, and P_{38}, respectively), were calculated following the method of Eugster and Michel [30] using the reported chemical compositions [17,18,20,21]. The method computes production rates for moderate shielding and then applies a moderation factor computed using the $(^{22}Ne/^{21}Ne)_C$ value. A moderation factor for ^{38}Ar production in achondrites was not specified [30], arguing that the dependence of P_{38} is negligible, in contrast to Cressy and Bogard [31] and Eugster [32], who proposed essentially similar shielding corrections. We corrected the P_{38} for shielding using the equation given by Eugster [32]. The calculated exposure ages are listed in Table 1 and those shown in Fig. 1 represent averages.

The CRE age of NWA817 of 10.0 ± 1.3 Ma is consistent with the 11 ± 0.9 Ma given by Eugster et al. [16] for the nakhlites (Fig. 1). The average exposure ages of 2.60 ± 0.21, 2.35 ± 0.20, and 2.01 ± 0.65 Ma for NWA856, NWA480, and NWA1068, respectively, agree well with the time of ejection from Mars of basaltic shergottites QUE94201, Shergotty and Zagami [16]. In contrast, the CRE age of 1.25 ± 0.07 Ma for SaU 005 is distinct from those of the other shergottites and is consistent with data reported by Pätsch et al. [23].

In addition to CRE ages based on He, Ne and Ar, we may assess the $^{15}N_C$ spallation data. The

Table 3
N concentrations and isotopic signatures in Martian meteorites studied here

Temp. (°C)	N (ppm)	δ^{15}N (‰)	Temp. (°C)	N (ppm)	δ^{15}N (‰)	Temp. (°C)	N (ppm)	δ^{15}N (‰)
Nakhlite NWA817, 131 mg			Shergottite NWA480, 187 mg			Shergottite SaU 005, 208 mg		
150	0.03	−3.9 ± 4.2	150	0.01	3.3 ± 5.2	150	0.01	−1.0 ± 2.6
250	1.12	4.0 ± 1.0	250	0.08	2.2 ± 2.4	250	1.03	−0.8 ± 1.1
300	0.59	2.6 ± 1.4	350	0.83	−0.6 ± 2.3	350	1.28	−2.4 ± 0.8
350	0.70	3.7 ± 1.7	500	0.86	5.1 ± 2.2	500	0.45	−7.6 ± 1.9
400	0.16	4.2 ± 1.6	450C	1.16	3.7 ± 1.9	450C	0.13	2.0 ± 1.6
450	0.15	2.9 ± 1.3	600	0.74	15.7 ± 1.3	600	0.15	14.4 ± 1.6
550	0.04	14.4 ± 4.9	700	1.37	14.4 ± 1.3	700	0.38	14.3 ± 1.5
700	1.07	33.5 ± 1.4	800	0.94	14.0 ± 1.3	800	0.36	13.1 ± 0.8
800	1.23	47.5 ± 1.2	900	0.32	14.5 ± 1.3	900	0.12	13.8 ± 1.0
900	1.30	57.0 ± 2.7	1000	0.086	14.6 ± 2.0	1000	0.08	14.0 ± 1.7
1000	0.76	43.1 ± 1.5	1200	0.055	59.5 ± 3.1	1200	0.06	55.0 ± 3.3
1200	0.32	85.9 ± 2.0	1400	0.050	88.9 ± 4.5	1400	0.04	54.2 ± 5.9
1400	0.19	126.8 ± 3.9	1550	0.013	80.6 ± 9.4	1550	0.01	−4.9 ± 5.8
1550	0.03	114.0 ± 8.6	Total	6.51	10.4 ± 1.7	Total	4.1	3.3 ± 1.2
Total	7.69	34.6 ± 1.7	Shergottite NWA1068, 287 mg					
Shergottite NWA856, 84 mg			150	0.01	1.6 ± 2.5			
150	0.03	3.4 ± 5.4	250	0.55	1.1 ± 1.4			
250	0.29	2.0 ± 2.1	350	1.14	3.1 ± 0.7			
350	0.34	3.6 ± 1.3	500	0.72	3.0 ± 0.9			
500	0.40	3.5 ± 1.2	450C	0.69	1.5 ± 1.1			
450C	0.57	1.5 ± 1.6	600	0.17	12.6 ± 1.5			
600	0.20	13.9 ± 2.6	700	2.21	22.0 ± 1.0			
800	0.73	41.4 ± 1.4	800	2.26	22.6 ± 1.1			
1000	0.34	43.6 ± 1.3	900	0.92	12.5 ± 1.2			
1200	0.06	105.0 ± 2.3	1000	0.43	12.8 ± 1.2			
1600	0.07	99.0 ± 4.9	1200	0.069	59.5 ± 3.9			
Total	3.03	21.5 ± 1.7	1400	0.066	74.8 ± 4.6			
			1600	0.009	72.3 ± 8.9			
			Total	9.24	14.7 ± 1.1			

C denotes a combustion step in O_2.

Table 4
Measured Xe isotopic ratios in NWA817, NWA480, NWA856, NWA1068, and SaU 005

Temp.(°C)	^{132}Xe	^{132}Xe = 1.00							
	(10^{-12} cm^3/g)	^{124}Xe	^{126}Xe	^{128}Xe	^{129}Xe	^{130}Xe	^{131}Xe	^{134}Xe	^{136}Xe
Nakhlite NWA817, 131 mg									
550	0.74	0.0033	0.0030	0.0724	0.99	0.1511	0.785	0.3877	0.3311
		± 12	13	23	6	24	14	36	32
700	1.59	0.0037	0.0040	0.0742	1.081	0.1527	0.7944	0.3852	0.3307
		± 8	10	14	21	15	68	23	21
800	3.04	0.0040	0.0042	0.0817	1.119	0.1599	0.8172	0.3959	0.3405
		± 6	6	10	11	12	58	20	19
1000	21.53	0.0133	0.0193	0.1014	1.169	0.1674	0.8392	0.4028	0.3420
		± 4	7	8	6	11	40	17	13
1200	18.56	0.0307	0.0478	0.1417	1.268	0.1890	0.8876	0.3992	0.3340
		± 5	6	9	6	10	41	19	14
1400	2.01	0.0125	0.0179	0.0986	1.638	0.1624	0.8360	0.4047	0.3446
		± 4	6	10	29	12	47	22	20
1550	0.50	0.0102	0.0138	0.0891	1.082	0.1612	0.8224	0.3942	0.3432
		± 11	14	17	24	19	100	35	32
Total	48.0	0.0189	0.0285	0.1141	1.217	0.1743	0.8539	0.4001	0.3384
Shergottite NWA480, 187 mg									
700	2.90	0.0035	0.0031	0.0718	0.97	0.1513	0.7921	0.3838	0.3302
		± 8	9	19	3	23	86	37	36
900	2.20	0.0037	0.0036	0.0734	1.08	0.1535	0.7932	0.3862	0.3333
		± 7	9	12	2	13	51	24	18
1000	0.73	0.0039	0.0041	0.0802	1.10	0.1577	0.8046	0.3976	0.3397
		± 8	10	16	2	17	68	27	20
1200	0.97	0.0137	0.0198	0.1036	1.19	0.1692	0.8263	0.3967	0.3356
		± 6	6	12	2	14	57	22	20
1400	2.56	0.0171	0.0254	0.1134	1.254	0.1810	0.8457	0.3986	0.3362
		± 6	6	10	24	11	48	20	17
1550	0.87	0.0118	0.0172	0.1021	1.06	0.1734	0.8243	0.3976	0.3348
		± 11	15	16	2	18	68	25	22
Total	10.2	0.0086	0.0116	0.0887	1.10	0.1632	0.8126	0.3914	0.3339
Shergottite NWA856, 84.1 mg									
1000	4.0	0.0048	0.0056	0.0858	1.047	0.1583	0.8078	0.3988	0.3411
		± 8	9	12	22	13	55	22	22
1500	21.3	0.0060	0.0066	0.0848	1.066	0.1590	0.8086	0.3983	0.3400
		± 4	4	9	5	9	45	16	14
Total	25.3	0.0058	0.0064	0.0850	1.063	0.1589	0.8085	0.3984	0.3402
Shergottite NWA1068, 287.1 mg									
800	3.14	0.0035	0.0032	0.0727	1.020	0.1523	0.7973	0.3886	0.3312
		± 7	8	12	21	13	56	25	21
1000	2.16	0.0051	0.0063	0.0841	1.120	0.1600	0.8267	0.4023	0.3432
		± 7	7	11	23	13	58	29	26
1200	1.93	0.0095	0.0125	0.0938	1.235	0.1640	0.8240	0.3971	0.3380
		± 6	7	12	21	12	66	24	19
1600	3.65	0.0075	0.0095	0.0891	1.219	0.1627	0.8252	0.3902	0.3308
		± 5	7	9	14	11	55	18	13
Total	10.9	0.0062	0.0076	0.0842	1.145	0.1594	0.8172	0.3934	0.3347

Table 4 (*Continued*).

Temp.(°C)	^{132}Xe	^{132}Xe = 1.00							
	(10^{-12} cm^3/g)	^{124}Xe	^{126}Xe	^{128}Xe	^{129}Xe	^{130}Xe	^{131}Xe	^{134}Xe	^{136}Xe
Shergottite SaU 005, 208 mg									
800	1.90	0.0035	0.0034	0.0719	1.02	0.1511	0.789	0.3916	0.3340
		± 5	4	12	3	12	6	25	21
1000	1.26	0.0033	0.0032	0.0786	1.06	0.1556	0.8066	0.3969	0.3390
		± 6	6	11	2	12	55	26	23
1400	3.89	0.0048	0.0042	0.0854	1.248	0.1642	0.8263	0.3867	0.3256
		± 4	3	9	24	10	47	21	18
1600	1.81	0.0063	0.0077	0.0886	1.051	0.1623	0.8174	0.3900	0.3279
		± 6	7	11	20	11	52	23	19
Total	8.9	0.0046	0.0046	0.0822	1.132	0.1598	0.8137	0.3899	00.3298

The ^{132}Xe are in units (10^{-12} cm^{3}STP/g). The extractions below 500°C (and a combustion step at 450°C) with terrestrial Xe are not included. Uncertainties listed are those in the least significant figures of the isotopic ratios (95% confidence levels).

$^{15}N_C$ production rates from oxygen are sensitive to low-energy secondaries and may constrain possible regolith exposures or break-up processes. The $^{15}N_C$ components are calculated relative to adopted indigenous nitrogen signatures and may, in turn, constrain the indigenous nitrogen component. We first calculate spallation $^{15}N_C$ amounts relative to the nitrogen signatures in the 1000°C step, with only minor spallation components (as in ALH84001, Chassigny and Nakhla [4,6]). The spallation $^{15}N_C$ components in the >1000°C steps are: 119 pg/g in NWA817, 30.9 pg/g in NWA856, 28.0 pg/g in NWA480, 30.6 pg/g in NWA1068, and 15.7 pg/g in SaU 005. These $^{15}N_C$ data, when coupled to an average lunar production rate of 11.6 pg/g/Ma [33], yield $^{15}N_C$ exposure ages listed in Table 1 (this 4π production rate fits those inferred from Chassigny, ALH84001, and Nakhla [4,6]). The $^{15}N_C$-based CRE ages are consistent with those based on ^{3}He, ^{21}Ne, and ^{38}Ar, and with those of Eugster et al. [34], who suggested that the nine shergottites required four ejection events, 0.73, 1.2, 2.7 and 19.8 Ma ago and inferred pre-atmospheric sizes of 0.2–2 m.

4. ^{40}K–^{40}Ar age systematics

The Ar isotopic abundances are corrected for the spallation components adopting the following ratios: $(^{36}Ar/^{38}Ar)_t = 5.3$, for interior Ar from Chassigny [4], and $(^{36}Ar/^{38}Ar)_C = 0.65$ [35], which is actually observed in the 1600°C step of NWA817. Alternatively, a ratio $(^{36}Ar/^{38}Ar)_t = 3.9$ [35] may be used for trapped Ar, but this yields similar $^{38}Ar_C$ and $^{36}Ar_t$ abundances (within ~5%). On the other hand, a 3% change in the adopted $(^{36}Ar/^{38}Ar)_C$ ratio changes the $^{36}Ar_t$ abundance of NWA480 by ~16%, and by ≤6% for other meteorites.

4.1. NWA817

The largest release of ^{40}Ar occurs at ~700°C, and >90% of ^{40}Ar is released between 600 and 1000°C, while only ~8% $^{38}Ar_C$ is observed in this temperature range. If $^{40}Ar = 2.04 \times 10^{-5}$ cm^{3}STP/g (450–1000°C steps) represents a pure radiogenic component, a K–Ar age of 1.36 Ga [K = 2657 ppm [17]) is calculated for NWA817. Alternatively, if all $^{36}Ar_t$ is assumed to represent a Martian atmospheric component ($^{40}Ar/^{36}Ar = 1800$), the calculated K–Ar age is reduced to 530 Ma. However, this option conflicts with the nitrogen and xenon signatures in NWA817 and is rejected. On the other hand, assuming that all $^{36}Ar_t$ represents either an ancient Martian atmospheric component of the type observed in ALH84001 or an interior Ar component of the type observed in Chassigny (both with $^{40}Ar/^{36}Ar \leq 200$ [4]), a K–Ar age of 1.36 Ga is estimated from the total ^{40}Ar. The ^{129}Xe excesses in NWA817, when assigned to a modern Martian atmospheric component ($^{40}Ar/^{129}Xe$ ratio of 1.4×10^6), yields a lower limit of 730 Ma for the K–Ar age, but if the ^{40}Ar/

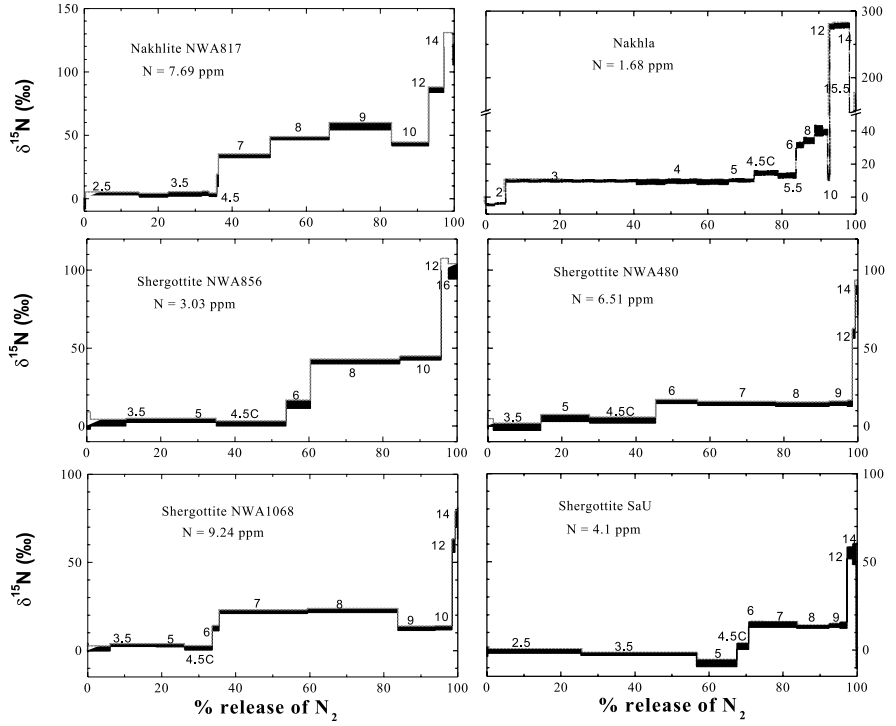

Fig. 2. The stepwise release of nitrogen from nakhlite NWA817, and from shergottites NWA480, NWA1068, NWA856, and SaU 005. Temperatures (in 100°C) are indicated. The low-temperature data reveal terrestrial nitrogen contamination ($\delta^{15}N = 2 \pm 2$‰). The plateau release in the temperature range >500 to 1000°C show the signature of indigenous N. The >1000°C data show significant shifts due to spallation ^{15}N components, which permit the calculation of CRE ages. These space exposure ages are consistent with CRE ages derived from noble gas data. For reference, the Nakhla release systematics [6] is included.

^{129}Xe ratio is fractionated by a factor of ~ 5 (similar to the $^{36}Ar/^{132}Xe$ ratio) then again a K–Ar age of 1.3 Ga is obtained. Since the radiometric ages of all nakhlites and also of Chassigny are consistent at 1.3 Ga, the NWA817 Ar data suggest that an atmospheric Ar component, if any, in NWA817 has $^{40}Ar/^{36}Ar$ ratios much lower than that in modern Martian atmosphere.

4.2. Shergottites

The shergottites release ^{40}Ar over a wider temperature range (600–1500°C) than nakhlite NWA817. If all ^{40}Ar is assigned to the radiogenic component, we calculate upper limits of 615 Ma, 790 Ma, 820 Ma, and 1.25 Ga [K = 830, 1079, 1328, and 183 ppm [18,21,20,22]) for the K–Ar ages of NWA480, NWA856, NWA1068, and SaU 005, respectively. If all $^{36}Ar_t$ in these shergottites is assigned to a modern Martian atmospheric component, then the calculated atmospheric ^{40}Ar components are larger than measured abundances. Thus most $^{36}Ar_t$ represents either indigenous Ar, or an early atmospheric component of the type observed in ALH84001 ($^{40}Ar/^{36}Ar < 200$ [4]). If $^{36}Ar_t$ represents an interior Ar component (of the type observed in Chassigny), K–Ar ages of 520, 670, 690, and 900 Ma are obtained for NWA480, NWA1068, NWA856, and SaU 005, respectively. We may assume a smaller contribution of modern Martian atmospheric Ar, limited by the observed excess ^{129}Xe. The $^{40}Ar/^{129}Xe$ ratio (1.4×10^6) of the modern atmosphere can be used to subtract such a component and lower limits of 315, 420, 490, and 620 Ma, for the K–Ar ages of NWA480, NWA1068, NWA856, and SaU 005, respectively, are derived. These lower limits are comparable to the reported

K–Ar age of Shergotty (480–530 Ma, [3]), but are significantly higher than radiometric ages of shergottites which fall into groups with 175 Ma (Shergotty has an Ar–Ar age of 167 Ma [36] and feldspar separates yielded a plateau Ar–Ar age of 250 Ma [37]) and 330–475 Ma [15]. Therefore, it appears that the shergottites studied here have inherited some ^{40}Ar from their source region, as is observed for fission Xe components (discussed later). It is likely that, during incorporation, the ^{40}Ar/^{129}Xe ratio became fractionated, and if fractionated by a factor of $\sim$5 (similar to those in the ^{36}Ar/^{132}Xe ratios), K–Ar ages of 485, 610, 650, 700 Ma (higher than radiometric ages) are estimated for NWA480, NWA1068, NWA856, and SaU 005, respectively. The $^{40}Ar_{atmospheric}$ component abundances derived above are strict upper limits (since all ^{129}Xe excesses are attributed to atmospheric component) and, therefore, the conclusion regarding inherited radiogenic ^{40}Ar appears robust.

5. Nitrogen isotopic composition

We now characterize Martian indigenous nitrogen components. The low-temperature nitrogen data (as well as the heavy noble gases) in meteorites recovered from hot deserts are compromised by terrestrial contamination. The data between 800 and 1000°C are useful for an analysis of the indigenous Martian N, as the spallation $^{15}N_C$ component appears predominantly in the $>$1000°C data (Table 3 and Fig. 2). The latter data show spallation $^{15}N_C$ components.

Nitrogen data at low temperatures ($\leq$500°C pyrolysis steps and 450°C combustion step) show a component slightly heavier ($\delta^{15}N = 2$–5‰; Table 3) than terrestrial atmospheric N, but consistent with contaminant signatures in terrestrial samples [38]. This component accounts for 30–50% of the total N. On the other hand, nitrogen signatures of SaU 005 reveal a light N component ($\delta^{15}N = -8$‰), as observed for indigenous Martian nitrogen (e.g. in Chassigny and ALH84001), but signatures in terrestrial weathering products like caliche [39] are similar.

A large number of observations on Holocene

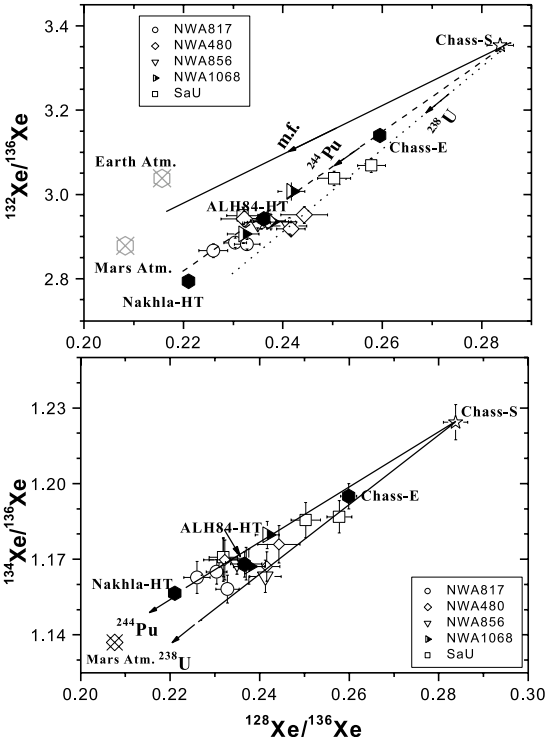

Fig. 3. The evidence for fission components is shown in two correlations. The upper panel shows the spallation-corrected ^{132}Xe/^{136}Xe ratios vs. ^{128}Xe/^{136}Xe. For reference, the terrestrial and Mars atmospheric composition [13] are shown; Chass-S and Chass-E represent the solar and evolved (fission plus solar) Xe components in Chassigny [4]. The lower panel shows the spallation-corrected isotopic ratios ^{132}Xe/^{136}Xe vs. ^{128}Xe/^{136}Xe. In both plots the addition of fission Xe due to ^{244}Pu and ^{238}U to Chass-S xenon are apparent. Most data fall along tie-lines of Chass-S and ^{244}Pu fission Xe, but in shergottites with low fission Xe concentrations (e.g. SaU 005 and NWA480) the shifts towards the ^{238}U fission end-member are apparent.

markers of humid conditions show that the Sahara was humid during most of the Holocene and the region experienced a drastic move to today's arid conditions following a series of climatic oscillations. The most abrupt episode started around 5.0 ka ago and aridity culminated at 3.8 ka ago and did not significantly change since then [40]. Note that most of the Xe released in the low-temperature steps (up to $\sim$700°C) represents terrestrial contamination. This contrasts with the rather small contamination levels observed in ALH84001, Chassigny and Nakhla.

The indigenous Martian nitrogen signatures are best documented in plateau releases in the range ~700–1000°C (Fig. 2). These signatures in NWA480 and SaU 005 (~50% and ~25% of total N, respectively) are uniform ($\delta^{15}N = \sim 14‰$) and consistent with the (evolved) N component in Chassigny [4]. In contrast, Nakhlite NWA817 and shergottite NWA856 release heavier N ($\delta^{15}N \sim 40–50‰$), comparable to the indigenous component in Nakhla ($\delta^{15}N = \sim 40‰$ [6]). While in Nakhla, evidence for modern Martian atmospheric Xe was reported [6–8], this source is not found in data of either nakhlite NWA817 or basaltic shergottite NWA856. Shergottite NWA1068 shows heavy N ($\delta^{15}N \sim 22‰$) but only in the 700 and 800°C steps, while the data of the 600, 900, and 1000°C steps ($\delta^{15}N = 13‰$) agree with those observed in NWA480 and SaU 005. These results suggest that two or more distinct nitrogen components are present in the source regions of shergottites and nakhlites.

Alternatively, the heavy N signatures in the intermediate steps may be affected by modern Martian atmospheric nitrogen. However, since nitrogen in the 700–1000°C steps is not accompanied by ^{129}Xe excesses of the modern (and ancient) Martian atmosphere, such a source is not likely.

6. Fission xenon components: identification in shergottites

All meteorites analyzed during this study show Xe isotopic excesses on the heavy isotopes that highlight the occurrence of fissiogenic xenon. Fig. 3 shows the correlations $^{132}Xe/^{136}Xe$ and $^{134}Xe/^{136}Xe$ vs. $^{128}Xe/^{136}Xe$, which allows a separation of the different Xe components. One end-member, Chass-S, was identified in low temperature of Chassigny and is thought to represent xenon from the Martian interior [3,4]. Also shown are the terrestrial and Martian atmospheric compositions, which are distinct from Chass-S xenon in this diagram. Contributions of fissiogenic Xe from ^{238}U and ^{244}Pu (see arrows in Fig. 3) are evident in Xe signatures (>1000°C steps) of Chassigny (Chass-E), Nakhla, and of ALH84001 [4,6]. These data plot on the ^{244}Pu fission mixing line rather than on the ^{238}U fission line, showing that fissiogenic Xe is mainly contributed by ^{244}Pu, a view fully consistent with the fission Xe concentrations (see below). Fission Xe components were recently also observed in EETA79001 and Shergotty [41].

We now evaluate the fission Xe components in the new shergottites and in nakhlite NWA817. Mathew and Marti [6] used the stepwise release

Table 5
The fission (compared to Chass-S Xe) and radiogenic ^{129}Xe excesses (compared to $^{129}Xe/^{132}Xe = 1.03$, the lowest measured ratio in Chassigny) in the Martian meteorites studied here

	^{132}Xe	$^{136}Xe_F$	U (ppb)	$^{136}Xe_U$	$^{129}Xe^*$	$^{136}Xe_F/^{136}Xe_U$	$^{129}Xe^*/^{136}Xe_F$	^{40}Ar	K (ppm)	K–Ar ages (Ma)
NWA817	42.6	28	136	1.05–4.64	9.28	26–7	3.3	23.4	2657	1300–1360
NWA480	5.1	2	64	0.11–2.18	0.67	9–1	3.4	2.35	830	315–520
NWA856	25.3	15	94	0.26–3.2	1.05	41–5	0.7	4.05	1079	490–690
NWA1068	7.7	4	100	0.23–3.41	1.36	21–1	3.2	5.22	1328	420–670
SaU 005	7.0	2	50	0.17–1.70	0.67	5–1	3.4	1.23	183	620–900
Nakhla [6]	8.3	7	56	0.43–1.91		16–4	6.4	7.37		
ALH84001 [4]	20.0	9	12	0.36–0.41	15.9	25–22	8.8			
Chassigny [4]	27.0	7	15	0.12–0.51	1.6	58–14	2.3			

K and U abundances are from Sautter et al. [17], Barrat et al. [18,21], Jambon et al. [20] and Dreibus et al. [22].
^{132}Xe abundances (>1000°C steps, since lower temperature extractions are affected by terrestrial Xe) and $^{129}Xe^*$ are in units 10^{-12} cm^3STP/g and the fission excesses are in units 10^{-13} cm^3STP/g. The lower and upper limits in the fission ^{136}Xe from ^{238}U fission are listed. These correspond to ^{238}U-produced fission Xe component during the lower K–Ar age and during an assumed age of 4.4 Ga. The ^{40}Ar abundances are in 10^{-6} cm^3STP/g units. The upper limits to the K–Ar ages are calculated assuming a Chassigny-type interior Ar component (with $^{40}Ar/^{36}Ar < 200$) and the lower limits in addition assume that all observed $^{129}Xe^*$ are modern Martian atmospheric-derived.

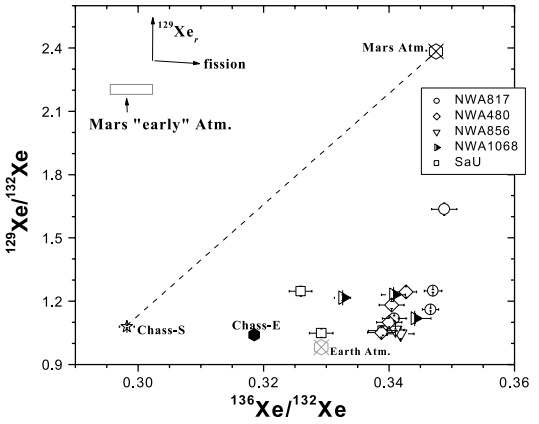

Fig. 4. Measured $^{136}Xe/^{132}Xe$ vs. $^{129}Xe/^{132}Xe$ isotopic ratios. Reference compositions are the same as in Fig. 3, with the addition of data for (solar-type) 'early Mars atmospheric' Xe in ALH84001. Expected shifts due to addition of fission Xe are indicated. Corrections due to a spallation component are minor for these isotopic ratios. Two-component mixtures of Chass-S and modern Martian atmospheric Xe or three-component mixtures (with terrestrial Xe as the third component) cannot explain the isotopic variations (see text).

systematics of Xe isotopes in Nakhla for disentangling indigenous and nucleogenic components. We use a similar approach for nakhlite NWA817, since the isotopic signatures show variations with temperature. First, the data show that the fission Xe component in the high-temperature (>1000°C) steps is well mixed with indigenous Xe as the two components are released together. In contrast, differential releases are observed for the cosmic-ray spallation component and for radiogenic $^{129}Xe_r$. The subtraction technique (1200°C step minus 1000°C step) permits the evaluation of the spallation Xe_C spectrum, which turns out to be consistent with that observed in Nakhla, indicating similar small shielding effects and consistent Ba/REE abundance ratios. We adopt the following spallation spectrum $^{124}Xe:^{126}Xe:^{128}Xe:^{129}Xe:^{130}Xe:^{131}Xe:^{132}Xe:^{134}Xe = 0.606 \pm 0.003 : \equiv 1.00 : 1.45 \pm 0.03 : 1.64 \pm 0.15 : 0.93 \pm 0.06 : 2.59 \pm 0.3 : 0.85 \pm 0.25 : 0.28 \pm 0.11$ [6] and report the spallation-corrected Xe isotope ratios in Appendix A[1]. For shergottites, because of their shorter exposure ages, the spallation corrections are smaller.

The spallation-corrected Xe data show in NWA817 as well as in all shergottites, isotopic shifts due to fission Xe components added to solar-type Xe (Chass-S). Fig. 3 shows that the fission component in nakhlite NWA817 carries the ^{244}Pu signature, while some temperature fractions of shergottites NWA480 and SaU 005 plot close to the ^{238}U fission Xe tie-lines, hence suggesting significant fission contribution from ^{238}U rather than ^{244}Pu. We calculate how much fissiogenic Xe could be produced from ^{238}U, during either the radiometric ages of the meteorites, or during a 4.4 Ga evolutionary time frame, based on the presence of extinct ^{244}Pu, which in the latter model survived the events recorded in radiometric ages. Results of such calculations confirm that the observed fission Xe excesses in NWA480 and SaU 005, and probably also in NWA1068, can largely be accounted for by fission Xe from decay of ^{238}U (Table 5). For other SNC, the ma-

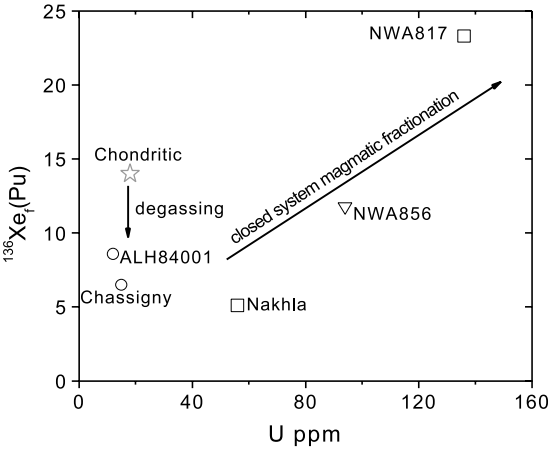

Fig. 5. This figure illustrates expected shifts due to degassing and magmatic fractionation. Concentrations of $^{136}Xe_f$ due to fission of ^{244}Pu (in 10^{-13} cm^3STP/g) vs. uranium abundances are plotted. The $^{136}Xe_f$ concentration does not include the component due to ^{238}U fission Xe produced during the past 4.4 Ga. The 'chondritic' data point corresponds to $^{136}Xe_f$ calculated for fission of ^{244}Pu in initially chondritic abundances and present-day ^{238}U in chondrites. The vertical arrows correspond to magma degassing and the 'magmatic fractionation' arrow illustrates the correlated evolution of $^{136}Xe_f$ and U in closed-system conditions, assuming that both are incompatible during magma differentiation.

[1] See online version of this paper.

jor fraction of fissiogenic Xe was contributed by ^{244}Pu (Table 5). Furthermore, nakhlite NWA817 reveals a uniform mixture of assimilated fission Xe into the indigenous component, as already observed in Nakhla [6]. Finally, Fig. 3 also shows that the Xe isotopic signatures in the high-temperature steps are not consistent with mixtures of mass-fractionated components (e.g. Martian atmospheric Xe) as the second end-member.

7. Time of differentiation: two-step model

To sum up the Xe isotopic results, SNCs, contain a well-homogenized mixture of indigenous Xe, presumably of interior origin, and of fissiogenic Xe, which in ALH84001, Chassigny, and the nakhlites and at least one shergottite is dominated by the extinct ^{244}Pu ($T_{1/2}$ = 82 Ma). The occurrence of such a fossil component has far-reaching implications that are discussed here in the framework of the early history of Mars as recorded by extinct radioactivities.

The fission component is well mixed with the indigenous interior component, as shown in Figs. 3 and 4. Such uniform mixing could be due to incorporating variable amounts of a xenon component having a near-constant proportion of ^{244}Pu-produced fission Xe relative to interior Xe. Alternatively, it could also result from magmatic differentiation when ^{244}Pu was still alive, provided that both interior Xe and Pu were incompatible elements during the course of magma evolution. With respect to this possibility, it is interesting to note that, for the two nakhlites, uranium and REE as proxies for Pu are enriched with respect to both chondrites and other SNC, and correlate with fission Xe (as well as with indigenous Xe; Fig. 5). Such coupled enrichments suggest that both incompatible and volatile elements have been concentrated through magma fractionation that led to the observed mineralogy and chemistry of nakhlites [17].

The early history of Mars as recorded in the decay products of radionuclides ^{146}Sm [1,42] and ^{182}Hf [1] in SNC document that the Martian mantle retained heterogeneities from the early, large-scale differentiation of Mars through magma ocean episodes. In particular, SNCs, including nakhlites and Chassigny, reveal ^{142}Nd anomalies that require fractionation of their source regions in order to get suprachondritic Sm/Nd ratios [42,43]. Such a suprachondritic ratio is not observed in the chemical composition of nakhlites and Chassigny, which, in contrast, present Sm/Nd ratios lower-than-chondritic and, therefore, require a two-stage evolution that can be summarized as follows. Large-scale mantle fractionation episodes took place within a few tens of Ma after start of solar system formation [1]. At some later stage (after decay of ^{146}Sm, half-life = 106 Ma), some local or regional magma differentiation settled the chemistry of nakhlites and of Chassigny. Such magmatism could either have happened very early, or about 1.3 Ga ago, if the radiometric ages of these meteorites in fact document magmatic episodes.

Modeling the Xe records of extinct radioactivities ^{129}I and ^{244}Pu in SNC, Marty and Marti [10]

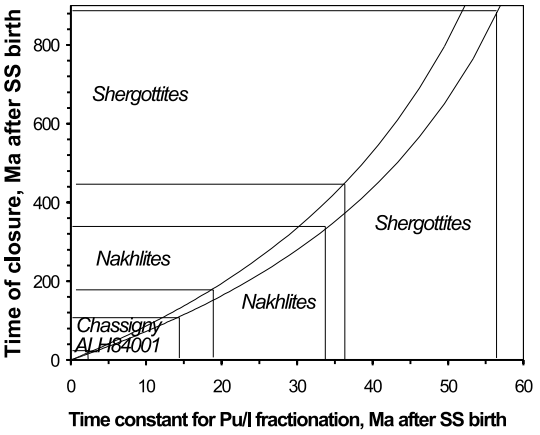

Fig. 6. The calculated 'Time of reservoir closure' vs. 'Time constant for Pu/I fractionation' (following Marty and Marti [10]). The former corresponds to the time necessary to allow decay of ^{244}Pu in open-system conditions, considering the amount of fissiogenic Xe left in analyzed SNCs (no ^{238}U fission correction was applied so that times of closure of shergottites are upper limits, whereas those of other SNCs are little affected since fissiogenic Xe is dominated by ^{244}Pu fission). The time constant of Pu/I fractionation is the time interval required to divide by a factor of 2 the Pu/I ratio of the Martian mantle, by extraction of volatile elements including iodine.

proposed a two-stage history for interior volatiles, with large-scale degassing and Pu/I fractionation taking place within the first 60 Ma, followed by residual mantle degassing that could have lasted several hundred Ma (Fig. 6).

Two types of scenarios can account for the occurrence of fissiogenic xenon from ^{244}Pu. In the first one, a xenon component consisting of fission products, assimilated to and mixed with interior Xe, was either added in variable proportions to each meteorite parent magma, or was fractionated to variable extent. In this case the magmatic fractionation that shaped the mineralogy of these meteorites could have taken place at any time after the decay of ^{244}Pu in the parent reservoirs. The only requirement in this scenario is that this assimilated xenon component survived, or even was acquired, during the 0.2–1.3 Ga metamorphic episodes that affected all known SNCs, except for ALH84001, despite resetting events for the K–Ar as well as Rb–Sr, Sm–Nd and U–Pb chronometers. A second, and more puzzling, scenario is that ^{244}Pu was still alive during the magmatic episodes, as suggested by the U–Xe_f correlated enrichments of nakhlites (Fig. 5). This scenario implies that magmatic fractionation took place early in Mars history, within the first few hundred Ma, and that the metamorphisms at 1.3 Ga and later were not magmatic. It also implies that the xenon component survived such episodes, in contrast to argon isotopic signatures, which were reset.

In both scenarios proposed above based on isotopic records, xenon has to be enriched in the nakhlite liquids during the course of magma differentiation, as the mixed indigenous and fission components correlate with incompatible elements like U or REE. Such closed-system conditions for noble gases require considerable pressure (depth) for the evolving liquids, although an exact depth cannot be assessed since magma degassing is controlled by the major volatile (H_2O and CO_2) contents, which are not known for Mars. This condition is nevertheless compatible with a recent study by Lentz et al. [44]. These authors studied elemental abundances of Li, Be and B to trace water–magma interactions and found differences between nakhlites and shergottites. They suggest that the evidence might indicate B and Li in pyroxenes were affected by a hot aqueous fluid in magma at depth >4 km, where water would remain dissolved in the parent magma.

The shergottites contain much less fissiogenic Xe than other SNCs and do not exhibit correlations between incompatible elements and either interior Xe or fissiogenic Xe (Table 5 and Fig. 5). Assuming that fission Xe contents below a chondritic reference value result from mantle source degassing (following Marty and Marti [10]), we use I/Pu ratios computed from measured $^{129}Xe^*/^{136}Xe_f$ ratios in shergottites studied here and model the implied time intervals characteristic of I/Pu evolution. We find that the time scale for 'primary' volatile/refractory fractionation is significantly longer than those calculated for ALH84001, Chassigny, and nakhlites (Fig. 6), and also that the time required for residual degassing of the Martian mantle is much longer, up to 1 Ga. Although model-dependent, these time scales suggest that the source regions of shergottites experienced dynamic histories that differed from those of other SNCs.

Fig. 4 illustrates that (with the possible exception of SaU 005) the mixing ratios of fission components and indigenous Chass-S xenon are very tightly constrained and that their resolution by stepwise release is not possible. This figure also shows that this uniformity in Xe mixtures does not extend to ^{129}Xe, since shifts up to $^{129}Xe/^{132}Xe = 1.64$ are observed in NWA817. In the context of the previous discussion of the fission components, we visualize two options for this variation: (1) a residue of either in situ produced $^{129}Xe_r$ from the decay of ^{129}I or an early trapping of the decay product in a refractory phase, which affects $^{129}Xe/^{132}Xe$ ratios measured predominantly at high temperatures; and (2) $^{129}Xe/^{132}Xe$ variations are due to mixing and incorporation of crustal or paleoatmospheric components with isotopic signatures of Chass-S (solar-type) xenon, except for ^{129}Xe. We note that variable $^{129}Xe/^{132}Xe$ ratios were also reported for temperature fractions (>1000°C) of Nakhla [6]. The shergottites NWA480, NWA1068, and SaU 005 show smaller, but nevertheless well-resolved $^{129}Xe/^{132}Xe$ variations too. In the former case (1), the $^{129}Xe_r$ component further constrains the timing of the initial

differentiation as ^{129}I was available only during the first ~100 Ma of Martian history.

8. Conclusions

1. The CRE age of nakhlite NWA817 (10.0 ± 1.3 Ma) is consistent with the ejection time of other nakhlites from Mars. The exposure ages of 2.60 ± 0.21 Ma, 2.35 ± 0.20 Ma, 2.01 ± 0.65 Ma, for NWA856, NWA480, NWA1068, respectively, are consistent with previously inferred ejection times for basaltic shergottites, but a lower CRE age of shergottite SaU 005 is confirmed.
2. The K–Ar ages of nakhlite NWA817 and of the shergottites NWA480, NWA856, NWA-1068, and SaU 005 are similar to ages reported in literature for the respective groups. The shergottite K–Ar ages, however, are older than the reported radiometric ages, indicating the incorporation of 'excess ^{40}Ar' into the lavas.
3. Distinct N signatures are identified in the Martian meteorites. Indigenous N in shergottites NWA480 and SaU 005 is consistent with the Chass-E (evolved) N signature ($\delta^{15}N = 13‰$). The indigenous N components in nakhlite NWA817 and in shergottite NWA856 are similar to indigenous N in Nakhla ($\delta^{15}N = 40‰$).
4. Fission Xe components due to ^{244}Pu are not only identified in nakhlite NWA817 but also in at least one shergottite. The observed fission excesses are higher by factors of 5–41, compared to the in situ produced ^{238}U fission component and are well mixed with indigenous Xe.
5. While the presence of a recent Martian atmospheric Xe component was inferred in some temperature steps of Nakhla, no such signature is present in nakhlite NWA817 and this allows the identification of radiogenic excess ^{129}Xe in the latter.

Acknowledgements

We thank the Théodore Monod consortium, in particular J.A. Barrat, for providing the samples and chemical analyses. We appreciate discussions with J.A. Barrat and V. Sautter on the petrology and magmatic history of these meteorites. We acknowledge helpful suggestions in reviews by D.D. Bogard and J.A. Whitby and support from NASA Grant NAG5-11554 and by grants from CNES and Conseil Régional de Lorraine.*[KF]*

References

[1] A.N. Halliday, H. Wänke, J.L. Birck, R.N. Clayton, The accretion, composition, and early differentiation of Mars, Space Sci. Rev. 96 (2001) 1–34.
[2] A.D. Brandon, R.J. Walker, J.W. Morgan, C.G. Goles, Re-Os isotopic evidence for early differentiation of the Martian mantle, Geochim. Cosmochim. Acta 64 (2000) 4083–4095.
[3] U. Ott, Noble gases in SNC meteorites: Shergotty, Nakhla, Chassigny, Geochim. Cosmochim. Acta 52 (1988) 1937–1948.
[4] K.J. Mathew, K. Marti, Early evolution of Martian volatiles: Nitrogen and noble gas components in ALH84001 and Chassigny, J. Geophys. Res. 106 (2001) 1401–1422.
[5] J.D. Gilmour, J.A. Whitby, G. Turner, Xenon isotopes in irradiated ALH84001: Evidence for shock-induced trapping of ancient Martian atmosphere, Geochim. Cosmochim. Acta 62 (1998) 2555–2571.
[6] K.J. Mathew, K. Marti, Martian atmospheric and interior volatiles in the meteorite Nakhla, Earth Planet. Sci. Lett. 199 (2002) 7–20.
[7] J.D. Gilmour, J.A. Whitby, G. Turner, Martian atmospheric xenon contents of Nakhla mineral separates: implications for the origin of elemental mass fractionation, Earth Planet. Sci. Lett. 166 (1999) 139–147.
[8] J.D. Gilmour, J.A. Whitby, G. Turner, Disentangling xenon components in Nakhla: Martian atmosphere, spallation and Martian interior, Geochim. Cosmochim. Acta 65 (2001) 343–354.
[9] M.J. Drake, T.D. Swindle, T. Owen, D.S. Musselwhite, Fractionated Martian atmosphere in the nakhlites, Meteoritics 29 (1994) 854–859.
[10] B. Marty, K. Marti, Signatures of early differentiation of Mars, Earth Planet. Sci. Lett. 196 (2002) 251–263.
[11] T.D. Swindle, M.W. Caffee, C.M. Hohenberg, Xenon and other noble gases in shergottites, Geochim. Cosmochim. Acta 50 (1986) 1001–1015.
[12] D.D. Bogard, D.H. Garrison, Relative abundances of argon, krypton, and xenon in the Martian atmosphere as measured in Martian meteorites, Geochim. Cosmochim. Acta 62 (1998) 1829–1835.
[13] K.J. Mathew, J.S. Kim, K. Marti, Martian atmospheric and indigenous components of xenon and nitrogen in the Shergotty, Nakhla, and Chassigny group meteorites, Meteorit. Planet. Sci. 33 (1998) 655–664.

[14] T.L. Segura, O.B. Toon, A. Colaprete, K. Zahnle, Environmental effects of large impacts on Mars, Science 298 (2002) 1977.
[15] L.E. Nyquist, D.D. Bogard, C.-Y. Shih, A. Greshake, D. Stöffler, O. Eugster, Ages and geologic histories of Martian meteorites, Space Sci. Rev. 96 (2001) 105–164.
[16] O. Eugster, A. Weigel, E. Polnau, Ejection times of Martian meteorites, Geochim. Cosmochim. Acta 61 (1997) 2749–2757.
[17] V. Sautter, J.A. Barrat, A. Jambon, J.P. Lorand, Ph. Gillet, M. Javoy, J.L. Joron, M. Lesourd, A new Martian meteorite from Morocco: the nakhlite North West Africa 817, Earth Planet. Sci. Lett. 195 (2002) 223–238.
[18] J.A. Barrat, Ph. Gillet, V. Sautter, A. Jambon, M. Javoy, C. Göpel, M. Lesourd, F. Keller, E. Petit, Petrology and chemistry of the basaltic shergottite North West Africa 480, Meteorit. Planet. Sci. 37 (2002) 487–499.
[19] H.Y. McSween Jr., D.D. Eisenhour, L.A. Taylor, M. Wadhwa, G. Crozaz, QUE94201 shergottite: Crystallization of a Martian basaltic magma, Geochim. Cosmochim. Acta 60 (1996) 4563–4569.
[20] A. Jambon, J.A. Barrat, V. Sautter, Ph. Gillet, C. Göpel, M. Javoy, J.L. Joron, M. Lesourd, The basaltic shergottite Northwest Africa 856: Petrology and Chemistry, Meteorit. Planet. Sci. 37 (2002) 1147–1164.
[21] J.A. Barrat, A. Jambon, M. Bohn, Ph. Gillet, V. Sautter, C. Göpel, M. Lesourd, F. Keller, Petrology and chemistry of the picritic shergottite North West Africa 1068, Geochim. Cosmochim. Acta 66 (2002) 3505–3518.
[22] G. Dreibus, B. Spettel, R. Haubold, K.P. Jochum, H. Palme, D. Wolf, J. Zipfel, Chemistry of a new shergottite: Sayh al Uhaymir 005 (abstract), Meteorit. Planet. Sci. 35 (2000) A49.
[23] M. Pätsch, M. Altmaier, U. Herpers, H. Kosuch, R. Michel, L. Schultz, Exposure age of the new SNC meteorite Sayh al Uhaymir 005 (abstract), Meteorit. Planet. Sci. 35 (2000) A124.
[24] F. Humbert, G. Libourel, C. France-Lanord, L. Zimmermann, B. Marty, CO_2-laser extraction-static mass spectrometry analysis of ultra-low concentrations of nitrogen in silicates, Geostand. Newsl. 24 (2000) 255–260.
[25] Y. Kim, Isotopic disequilibrium in the Acapulco parent body: observed components and genetic relationship to other meteorites, Ph.D. Thesis, University of California, San Diego (1994).
[26] J.N. Head, H.J. Melosh, B.A. Ivanov, Martian meteorite launch: High-speed ejecta from small craters, Science 298 (2002) 1752–1756.
[27] B. Marty, K. Marti, J.A. Barrat, J.L. Birck, J. Blichert-Toft, M. Chaussidon, E. Deloule, P. Gillet, C. Göpel, A. Jambon, G. Manhes, V. Sautter, Noble gases in new SNC meteorites NWA817 and NWA480 (abstract), Meteorit. Planet. Sci. 36 (2001) A122–A123.
[28] F. Begemann, L. Schultz, The influence of bulk chemical composition on the production rate of cosmogenic nuclides in meteorites (abstract). Lunar and Planetary Sci. Conf. XIX (1988) 51–52.
[29] D.H. Garrison, M.N. Rao, D.D. Bogard, Solar-proton-produced neon in shergottite meteorites and implications for their origin, Meteoritics 30 (1995) 738–747.
[30] O. Eugster, Th. Michel, Common asteroid break-up events of eucrites, diogenites, and howardites and cosmic-ray production rates for noble gases in achondrites, Geochim. Cosmochim. Acta 59 (1995) 177–199.
[31] P.J. Cressy, D.D. Bogard, On the calculation of cosmic-ray exposure ages of stone meteorites, Geochim. Cosmochim. Acta 40 (1976) 749–762.
[32] O. Eugster, Cosmic-ray production rates for ^{3}He, ^{21}Ne, ^{38}Ar, ^{83}Kr, and ^{126}Xe in chondrites based on ^{81}Kr-Kr exposure ages, Geochim. Cosmochim. Acta 52 (1988) 1649–1662.
[33] K.J. Mathew, K. Marti, Lunar nitrogen: indigenous signature and cosmic-ray production rate, Earth Planet. Sci. Lett. 184 (2001) 659–669.
[34] O. Eugster, H. Busemann, S. Lorenzetti, D. Terribilini, Ejection ages from krypton-81-krypton-83 dating and pre-atmospheric sizes of Martian meteorites, Meteorit. Planet. Sci. 37 (2002) 1345–1360.
[35] D.D. Bogard, A reappraisal of the Martian ^{36}Ar/^{38}Ar ratio, J. Geophys. Res. 102 (1997) 1653–1661.
[36] D.D. Bogard, D.H. Garrison, Argon-39-argon-40 'ages' and trapped argon in Martian shergottites, Chassigny, and Allan Hills 84001, Meteorit. Planet. Sci. 34 (1999) 451–473.
[37] D.D. Bogard, L. Husain, L.E. Nyquist, ^{40}Ar-^{39}Ar age of the Shergotty achondrite and implications for its post-shock thermal history, Geochim. Cosmochim. Acta 43 (1979) 1047–1055.
[38] B. Marty, F. Humbert, Nitrogen and argon isotopes in oceanic basalts, Earth Planet. Sci. Lett. 152 (1997) 101–112.
[39] S.P. Schwenzer, R.K. Mohapatra, U. Ott, Nitrogen and noble gases in caliche from the Martian meteorite SaU 008, Geochim. Cosmochim. Acta 66 (2002) A693.
[40] N. Petit-Maire, Z. Guo, Mise en évidence de variations climatiques holocènes rapides, en phase dans les déserts actuels de Chine et du Nord de l'Afrique, C. R. Acad. Sci. Paris Ser. IIa (1996) 847–851.
[41] K.D. Ocker, J.D. Gilmour, Martian atmospheric and 'interior' xenon components in EETA79001 Lith-B mineral separates (abstract), Lunar and Planet. Sci. XXXIII (2002) CD-ROM, #1603.
[42] E. Jagoutz, Nd isotopic systematics of Chassigny (abstract), Lunar Planet. Sci. XXVII (1996) 597–598.
[43] N. Nakamura, D.M. Unruh, M. Tatsumoto, R. Hutchison, Origin and evolution of the Nakhla meteorite inferred from Sm-Nd and U-Pb systematics and REE, Ba, Sr, Rb abundances, Geochim. Cosmochim. Acta 46 (1982) 1555–1573.
[44] R.C.F. Lentz, H.Y. McSween, J. Ryan, L.R. Riciputi, Water in martian magmas: Clues from light lithophile elements in shergottite and nakhlite pyroxenes, Geochim. Cosmochim. Acta 65 (2001) 4551–4565.